

# Thermal tuning of phononic bandstructure in ferroelectric ceramic/epoxy phononic crystal

Cite as: Appl. Phys. Lett. **94**, 193501 (2009); <https://doi.org/10.1063/1.3136752>

Submitted: 04 March 2009 . Accepted: 24 April 2009 . Published Online: 12 May 2009

K. L. Jim, C. W. Leung, S. T. Lau, S. H. Choy, and H. L. W. Chan



View Online



Export Citation

## ARTICLES YOU MAY BE INTERESTED IN

[Tunable magnetoelastic phononic crystals](#)

Applied Physics Letters **95**, 124104 (2009); <https://doi.org/10.1063/1.3236537>

[Band gap tunability of magneto-elastic phononic crystal](#)

Journal of Applied Physics **111**, 054901 (2012); <https://doi.org/10.1063/1.3687928>

[Temperature effects on the band gaps of Lamb waves in a one-dimensional phononic-crystal plate \(L\)](#)

The Journal of the Acoustical Society of America **129**, 1157 (2011); <https://doi.org/10.1121/1.3543970>

Lock-in Amplifiers

Find out more today



Zurich Instruments

# Thermal tuning of phononic bandstructure in ferroelectric ceramic/epoxy phononic crystal

K. L. Jim, C. W. Leung,<sup>a)</sup> S. T. Lau, S. H. Choy, and H. L. W. Chan

Department of Applied Physics and Materials Research Centre, The Hong Kong Polytechnic University, Hung Hom, Kowloon, Hong Kong, People's Republic of China

(Received 4 March 2009; accepted 24 April 2009; published online 12 May 2009)

Thermal tuning of phononic bandgaps in megahertz range was demonstrated in ferroelectric ceramic-based phononic crystal structure. Temperature variation across ferroelectric phase transition, accompanied by substantial changes in acoustic velocities, leads to a shift in the phononic bandstructure of a two-dimensional (Ba,Sr)TiO<sub>3</sub>/epoxy composite sample over a range of 10 °C. Experimental results are supported by modelings based on plane-wave expansion calculations. The high tunability of phononic bandstructure is advantageous for active control of ultrasound transmissions. © 2009 American Institute of Physics. [DOI: 10.1063/1.3136752]

Analogous to electronic bandstructures in solids, it is possible to prepare artificial lattices with forbidden ranges of quasiparticle transmissions. Such bandgap “crystals” have been postulated and realized for electromagnetic waves (photons),<sup>1</sup> mechanical vibrations (phonons),<sup>2,3</sup> as well as collective spin fluctuations (magnons).<sup>4</sup> The ability to manipulate the propagation of such quasiparticles is crucial for the design of various devices.

In case of phononic crystals (PnCs), the effect has been demonstrated in audible,<sup>2</sup> ultrasonic,<sup>3</sup> and hypersonic frequencies.<sup>5,6</sup> For enhanced functionality, it is desirable to have an *active* control on the bandstructure,<sup>5</sup> ideally within the same fabricated sample. While numerous studies have been performed on tunable photonic crystals,<sup>7</sup> there are relatively few attempts to investigate tunable PnCs. In some reports, phononic bandgaps were changed either by mechanical motion or deformation of PnCs,<sup>8</sup> which are not ideal as compared to solid-state tuning schemes. For the latter category, Yang and Chen<sup>9</sup> studied changes in acoustical transmission by inducing strains in an array of dielectric elastomer tubes placed in air, through the application of an electric field. Huang and Wu,<sup>10</sup> on the other hand, investigated the influence of thermal expansion in quartz on the behavior of phononic gaps. Large stimuli are often required to produce modest changes in these examples.

Here we report calculations and experimental verification of a tunable ferroelectric/epoxy PnC composite structure in the ultrasonic range, based on changes in acoustic velocities during the phase transition of ferroelectric Ba<sub>0.7</sub>Sr<sub>0.3</sub>TiO<sub>3</sub> (BST). Perovskite ferroelectrics undergo phase transformation around Curie temperature ( $T_C$ ), generally accompanied by anomalies in material parameters such as dielectric constants and acoustic velocities.<sup>11</sup> For example, BaTiO<sub>3</sub> is an archetypal ferroelectric with a tetragonal-to-cubic transition at  $T_C=403$  K.<sup>12</sup> By replacing Ba<sup>2+</sup> with Sr<sup>2+</sup>,  $T_C$  of the material can be continuously tuned; for BST it has  $T_C\sim 35$  °C,<sup>13</sup> which is convenient for device operations. Measurements on PnCs were compared with calculations based on the corresponding material parameters below and above the  $T_C$  of BST. The high sensitivity of phononic bandstructure around  $T_C$  at megahertz range provides a simple

scheme for applications such as signal filtering, frequency-selective transducers, and tunable guidance of acoustic waves in slab waveguides,<sup>14</sup> in the fields such as industrial nondestructive testing and medical diagnoses and imaging.<sup>15</sup>

The acoustical dispersion relations in a solid medium can be calculated from the equation of motion, which governs the (position-dependent) lattice displacement in a linear medium

$$\rho \frac{\partial^2 u_i}{\partial t^2} = \nabla \cdot (\rho c_t^2 \nabla u_i) + \nabla \cdot \left( \rho c_l^2 \frac{\partial \mathbf{u}}{\partial x_i} \right) + \frac{\partial}{\partial x_i} [(\rho c_l^2 - 2\rho c_t^2) \nabla \cdot \mathbf{u}], \quad (1)$$

where  $\rho(\mathbf{r})$  is the density of the medium and  $\mathbf{u}$  is the displacement vector. For a two-dimensional (2D) PnC exhibiting spatial periodicity,  $\rho$ ,  $c_t$  and  $c_l$  (transverse and longitudinal acoustic velocities, respectively) can be expanded as a Fourier series. In case of a binary (BST and epoxy) composite with volume occupancies  $f$  and  $(1-f)$  in the unit cell, the Fourier coefficients can be calculated accordingly.

Material parameters for both BST and epoxy as functions of temperature were measured, in order to perform calculations based on Eq. (1).  $c_t$  and  $c_l$  in BST and epoxy (Epotek 301) were obtained by ultrasound through-transmission measurements.<sup>16</sup> Silicone oil ( $c_{\text{oil}}=998$  ms<sup>-1</sup> at 24 °C, which decreases monotonically to 925 ms<sup>-1</sup> at 50 °C) was used to improve the coupling of ultrasound to the samples (disks of diameter 20 mm and thickness 2.38 mm). Broadband pulses (duration  $\sim 300$  ns) were sent normally to sample surfaces, and the time lapse between the source and the receiver was used to calculate  $c_l$ . For  $c_t$ , transverse vibrations were triggered in samples based on the fact that  $c_{\text{oil}} < c_t < c_l$ . By impinging pulses at a specific range of angles, only transverse waves propagated through the samples while longitudinal waves were reflected.  $c_t$  was then obtained by  $c_t = (c_{\text{oil}}/\sin \theta) \sin[\tan^{-1}(d \sin \theta/d \cos \theta + \Delta t c_{\text{oil}})]$ , where  $d$  denotes the sample thickness and  $\Delta t$  the time difference between measurements with and without samples.<sup>16</sup>

Figure 1 shows the temperature dependence of  $c_l$  and  $c_t$  in BST, and the results at 35 and 45 °C are summarized in Table I. Drastic increases in acoustic velocities (21% and 29% for  $c_l$  and  $c_t$ , respectively) occurred when the tempera-

<sup>a)</sup>Electronic mail: apleung@polyu.edu.hk.

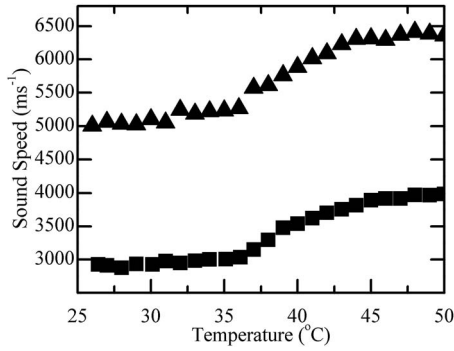


FIG. 1. Longitudinal (▲) and transverse (■) sound velocities in BST at various temperatures, as measured by the method described in Ref. 16.

ture changed from 35 to 45 °C; this temperature range overlaps with  $T_C$  of BST,<sup>13</sup> and the measured velocities are consistent with the results in literature.<sup>11</sup> For epoxy, a linear and minimal velocity change ( $<0.03\%$  for both  $c_l$  and  $c_t$ ) was recorded over the same temperature range.

BST/epoxy PnC sample was prepared by a dice-and-fill technique.<sup>17</sup> A polycrystalline BST ceramic disk (diameter 20 mm and thickness 2.38 mm) was fabricated by standard solid-state reaction processes. It was diced on the surface by a diamond blade with a wafer dicing saw, leaving behind 200- $\mu\text{m}$ -wide BST strips with a periodicity of 265  $\mu\text{m}$ . Epoxy was then filled in between the strips, and the sample was degassed in a vacuum chamber for 30 min before it was cured at 40 °C for another 30 min. Subsequently the sample surface was diced in the direction orthogonal to the original strips with the same periodicity. Epoxy was filled into the grooves, and the sample was degassed for another 30 min before curing for 12 h at 40 °C. A final grinding process removed excess BST and epoxy from both sides of the sample, leaving behind a 2D structure with square BST rods embedded in the epoxy matrix [inset, Fig. 2(a)]. We note that for the fabrication of smaller structures (such as hypersonic PnCs), the dice-and-fill technique cannot be used, and more advanced techniques (such as self-assembly of nanoparticles<sup>5</sup> or interference lithography<sup>6</sup>) have to be employed.

To verify the existence of phononic bandgaps, one can measure the transmission spectrum of acoustic waves across the samples. However, it is difficult to obtain clear signals and unambiguous interpretations by the transmission technique, as scattering and absorption can also result in suppressed signal transmission. Reflection measurements can yield information that can be readily comparable with calculated phononic bandstructures, as peaks in the reflection spectrum are clear signs of forbidden transmission through the samples. The reflection spectra of the PnC sample were therefore measured, employing an ultrasound pulse-echo method.

TABLE I. Measured  $c_s$  and  $c_t$  in BST and Epotek 301 at 35 and 45 °C.

Temperature (°C)	BST ( $\rho=3050 \text{ kg m}^{-3}$ )		Epoxy (Epotek 301) ( $\rho=1130 \text{ kg m}^{-3}$ )	
	$c_t$ ( $\text{ms}^{-1}$ )	$c_l$ ( $\text{ms}^{-1}$ )	$c_t$ ( $\text{ms}^{-1}$ )	$c_l$ ( $\text{ms}^{-1}$ )
35	3008	5233	1180	2580
45	3892	6317	1150	2530

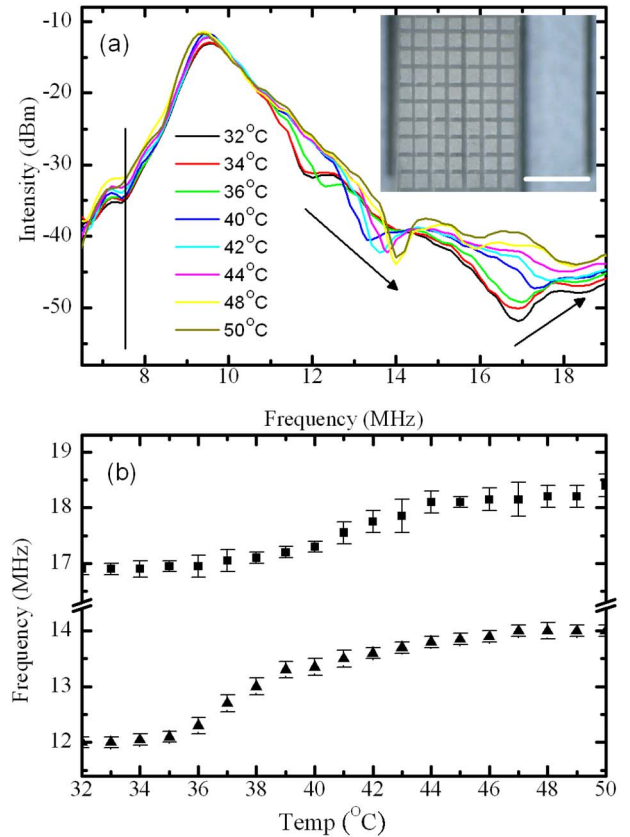


FIG. 2. (Color online) (a) Reflection spectra of BST/epoxy PnC at different temperatures. The temperature-independent dip at 7.5 MHz is highlighted by a vertical line, and the temperature dependences of the two dips in the reflection spectra are highlighted by arrows. Inset: photo of PnC sample tested in this work (scale bar=1 mm). (b) Temperature dependence of dip locations around 12–14 MHz (▲) and 17–18.5 MHz (■).

During measurements, the sample was immersed in a temperature-controlled water bath [sound speed varies between 1494 (24 °C) and 1540  $\text{ms}^{-1}$  (50 °C)].<sup>18</sup> A transducer (diameter 1 mm and central frequency 10 MHz) was used as both the transmitter and the receiver, and was placed 1 cm away from the sample. Ultrasound pulses were sent within the plane of the sample, along the direction in which the BST was diced. Reflected signals were amplified by an ultrasonic analyzer before displayed on an oscilloscope, which was fast Fourier transformed to obtain the reflection spectrum.

Figure 2(a) shows the temperature-dependent reflection spectra. A clear peak is obtained at 9.5 MHz. It is sandwiched between two dips, one of which is located at 7.5 MHz and unaffected by temperature. The dip at higher frequency, on the other hand, increases from 12 to 14 MHz. Similar temperature dependence of dip position occurs in between 17 and 18.5 MHz. Such changes are observed within a small temperature window from 35 to 45 °C [Fig. 2(b)], which coincides exactly with the temperature range in which changes in  $c_l$  and  $c_t$  in BST occur. The observed shift of dip positions suggests a strong correlation with the phase transition in BST. We have performed the measurements with both increasing and decreasing temperatures, and no hysteric behavior in dip positions was observed. The absence of hysteric behavior was also observed in the anomalous dielectric constant behavior of a BST ceramic over the same temperature range (data not shown). On the other hand,

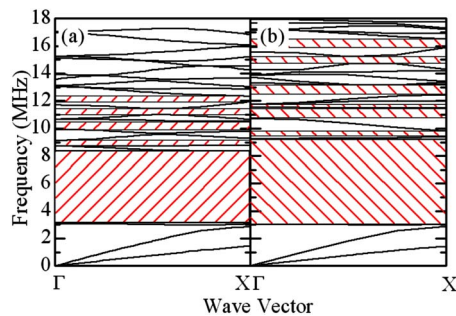


FIG. 3. (Color online) Computed dispersion relations of PnCs at 35 (a) and 45 °C (b), modeled with the same unit cell dimensions as the PnC sample used in this work. Only mixed modes along the  $\Gamma$ -X direction are shown. The positions of the phononic bandgaps are shaded.

no similar reflection dips in proximity with those mentioned above were found from control measurements on plain BST and epoxy disks across the same temperature range. We therefore argue that the dips at 12–14 and 17–18.5 MHz arise from variations in PnC structure. These correspond to upshift of bandedge by 17% (9%), over a narrow temperature range of 10 °C, for the dip at 12–14 MHz (17–18.5 MHz).

Bandstructure calculations were performed based on Eq. (1) by the plane-wave expansion (PWE) method,<sup>19</sup> and an infinite PnC structure is assumed. Figure 3 shows the calculated bandstructures at 35 [Fig. 3(a)] and 45 °C [Fig. 3(b)], using the corresponding experimental parameters of BST and epoxy in Table I. Notice that only mixed-mode propagation (i.e., combined longitudinal and in-plane transverse waves)<sup>19</sup> along  $\Gamma$ -X direction is shown. As the experiment was performed with ultrasound pulses hitting head-on to the sample along the dicing direction, it is expected that mixed-mode waves were predominately excited during measurements.

Two features are apparent in the figure. First, the lowest bandedge at  $\sim 3$  MHz is independent of temperature. This resembles the temperature-independent behavior of the dip at 7.5 MHz in Fig. 2(a). Besides, there is an upward shift of other bandedges with increasing temperature. This is qualitatively consistent with the observation in Fig. 2(a) for the frequency upshift of reflection dips. The expansion of bandgaps into the range 12.3–16.5 MHz with increasing temperatures also fits well with the observed increase in reflected signals at  $\sim 17$  MHz in Fig. 2(a). Notice that flat bandstructures in between the two gaps imply a very small phase velocity and thus ineffective coupling of acoustic waves into the sample. This, together with the fact that the resonant frequency of the transducer is  $\sim 9.5$  MHz, explains the absence of some dips in the reflection spectra, particularly around the main peak at 10 MHz.

Caution has to be exercised when interpreting the correlations between Figs. 2(a) and 3. Since an infinite array of unit cells was assumed in PWE calculations, bandgaps obtained in Fig. 3 indicate regions for complete blockage of phonon transmissions. That is, the gap positions are well defined, with complete reflections of incoming signals. Deviations from this ideal situation (finite number of unit cells,

structural artifacts, and imperfections) may lead to widened and less-pronounced gaps. Besides, we have defined the position of reflection spectra dips as bandgap edges for experimental convenience. It is impossible to draw quantitative links between Figs. 2(a) and 3 concerning the phononic bandstructure. Yet the identical trends in the two figures evidenced the realization of thermal tuning in phononic bandstructure.

In conclusion, we demonstrated strong tunability in BST/epoxy composite PnC structure, which matched theoretical calculations qualitatively. The high thermal sensitivity of acoustic velocities across  $T_C$ , together with the tunability of  $T_C$  by appropriate doping and their high structural stability, makes ferroelectric ceramics highly suitable for tunable phononics applications. The strong shift of phononic bandstructures at megahertz range around ambient temperature demonstrated by the present work can find immediate applications in various device schemes.

Financial support by Hong Kong Polytechnic University (Grant No. 1-BB9P) is acknowledged.

- <sup>1</sup>S. John, *Phys. Rev. Lett.* **58**, 2486 (1987); E. Yablonovitch, *ibid.* **58**, 2059 (1987).
- <sup>2</sup>J. V. Sánchez-Pérez, D. Caballero, R. Martínez-Sala, C. Rubio, J. Sánchez-Dehesa, F. Meseguer, J. Llinares, and F. Gálvez, *Phys. Rev. Lett.* **80**, 5325 (1998).
- <sup>3</sup>R. H. Olsson III and I. El-Kady, *Meas. Sci. Technol.* **20**, 012002 (2009); F. R. Montero de Espinosa, E. Jiménez, and M. Torres, *Phys. Rev. Lett.* **80**, 1208 (1998).
- <sup>4</sup>M. Krawczyk, J.-C. Lévy, D. Mercier, and H. Puzskarski, *Phys. Lett. A* **282**, 186 (2001).
- <sup>5</sup>W. Cheng, J. J. Wang, U. Jonas, G. Fytas, and N. Stefanou, *Nature Mater.* **5**, 830 (2006).
- <sup>6</sup>T. Gorishnyy, C. K. Ullal, M. Maldovan, G. Fytas, and E. L. Thomas, *Phys. Rev. Lett.* **94**, 115501 (2005).
- <sup>7</sup>K. L. Jim, D. Y. Wang, C. W. Leung, C. L. Choy, and H. L. W. Chan, *J. Appl. Phys.* **103**, 083107 (2008); M. Roussey, M. P. Bernal, N. Courjal, and F. I. Baida, *Appl. Phys. Lett.* **87**, 241101 (2005); M. Haurylau, S. P. Anderson, K. L. Marshall, and P. M. Fauchet, *ibid.* **88**, 061103 (2006).
- <sup>8</sup>L. Feng, X. P. Liu, M. H. Lu, Y. B. Chen, Y. F. Chen, Y. W. Mao, J. Zi, Y. Y. Zhu, S. N. Zhu, and N. B. Ming, *Phys. Rev. B* **73**, 193101 (2006); K. Bertoldi and M. C. Boyce, *ibid.* **77**, 052105 (2008).
- <sup>9</sup>W. P. Yang and L. W. Chen, *Smart Mater. Struct.* **17**, 015011 (2008).
- <sup>10</sup>Z. G. Huang and T. T. Wu, *IEEE Trans. Ultrason. Ferroelectr. Freq. Control* **52**, 365 (2005).
- <sup>11</sup>C. B. Parker, J.-P. Maria, and A. I. Kingon, *Appl. Phys. Lett.* **81**, 340 (2002); A. Moreno-Gobbi, D. Garcia, J. A. Eiras, and A. S. Bhalla, *Ferroelectrics* **337**, 197 (2006).
- <sup>12</sup>M. Radecka and M. Rekas, *J. Therm. Anal. Calorim.* **88**, 731 (2007).
- <sup>13</sup>D. Y. Wang, Y. Wang, X. Y. Zhou, H. L. W. Chan, and C. L. Choy, *Appl. Phys. Lett.* **86**, 212904 (2005).
- <sup>14</sup>R. Sainidou and N. Stefanou, *Phys. Rev. B* **73**, 184301 (2006).
- <sup>15</sup>K. K. Shung and M. Zippuro, *IEEE Eng. Med. Biol. Mag.* **15**, 20 (1996); G. R. Lockwood, D. H. Turnbull, D. A. Christopher, and F. S. Foster, *ibid.* **15**, 60 (1996).
- <sup>16</sup>R. J. Freemantle and R. E. Challis, *Meas. Sci. Technol.* **9**, 1291 (1998).
- <sup>17</sup>H. Taunaumang, I. L. Guy, and H. L. W. Chan, *J. Appl. Phys.* **76**, 484 (1994).
- <sup>18</sup>W. Marczak, *J. Acoust. Soc. Am.* **102**, 2776 (1997).
- <sup>19</sup>M. S. Kushwaha, P. Halevi, G. Martínez, L. Dobrzynski, and B. Djafari-Rouhani, *Phys. Rev. B* **49**, 2313 (1994).